



Bachelor Project

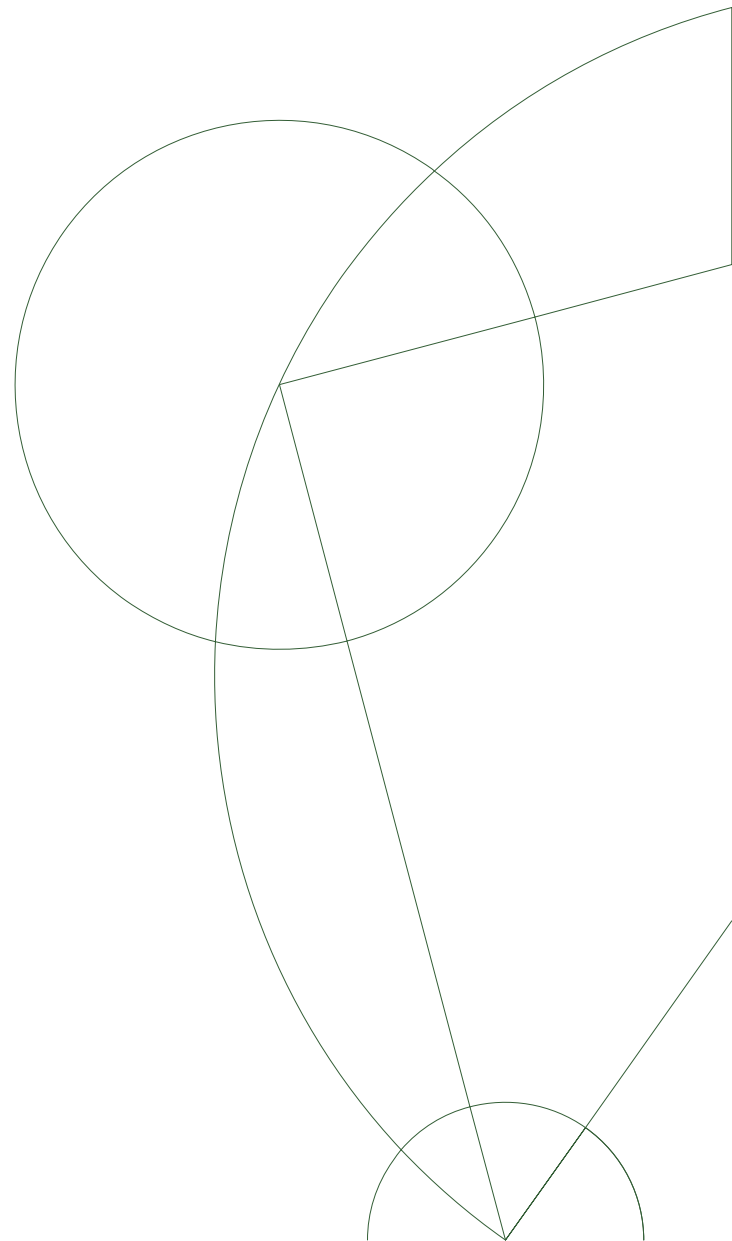
Extracting Anomalous Triple Gauge Boson Couplings at LHC for WZ

Alexander Pedersen Lind

pln879@alumni.ku.dk

Academic Advisor: Jørgen Beck Hansen

Submitted: June 11, 2014



Abstract

The aim of this project is to investigate the effect of the anomalous triple gauge boson couplings Δg_1^Z , $\Delta \kappa_Z$ and λ_Z on the kinematic variables by utilization of the Optimal Observables method. This is done by using 2598 $W^\pm Z^0$ events selected from proton-proton collisions with a center of mass energy of $\sqrt{s} = 8$ TeV and an integrated luminosity of $\int \mathcal{L} dt = 20.28 \text{ fb}^{-1}$ recorded with the ATLAS experiment in 2012. It is found that the process $pp \rightarrow l' \nu_l l^\pm l^\mp$, by applying appropriate selection cuts, will lead to a nearly clean signal of WZ events. Monte Carlo samples simulated to include TGCs has been used to compare with the data. This project presents an investigation of the Optimal Observables analysis method in the context of hadron colliders. The Optimal Observables for the three anomalous coupling parameters show strong sensitivity to the anomalous couplings with the $OO(\Delta g_1^Z)$ distribution appearing to be the least sensitive to the anomalous TGCs.

Resumé på dansk

Formålet med dette projekt er at undersøge effekten af de anormale tre-boson koblinger Δg_1^Z , $\Delta \kappa_Z$ og λ_Z på de kinematiske variable ved benyttelse af Optimale Observable metoden. Dette er gjort ved at benytte 2598 $W^\pm Z^0$ begivenheder selekteret fra proton-proton sammenstød med en masse midtpunktsenergi på $\sqrt{s} = 8$ TeV og en integreret luminositet på $\int \mathcal{L} dt = 20.28 \text{ fb}^{-1}$ målt med ATLAS eksperimentet i 2012. Der bliver fundet at processen $pp \rightarrow l' \nu_l l^\pm l^\mp$ giver, med passende udvælgelseskrav, et næsten rent signal af WZ begivenheder. Monte Carlo prøver, som er simuleret til at inkludere tre-boson koblinger, er blevet benyttet til sammenligning med data. Dette projekt præsenterer en undersøgelse af Optimale Observable analyse metoden i forbindelse med hadron kollisionseksperimenter. De Optimale Observable for de tre anormale kobling parametre udviser stærk følsomhed for de anormale koblinger, hvor $OO(\Delta g_1^Z)$ distributionen ser ud til at være den mindst følsomme over for de anormale tre-boson koblinger.

Contents

1	Introduction	1
2	Theoretical Background	1
2.1	The Standard Model	1
2.2	Quantum Field Theory	3
2.2.1	From classical physics to QFT and Lagrangian formalism	3
2.2.2	The Feynman Path Integral	4
2.2.3	Feynman Rules and Diagrams	4
2.2.4	Renormalization	6
2.2.5	Symmetries	6
2.2.6	Quantum Electrodynamics	7
2.2.7	Electroweak theory	8
2.3	Anomalous Triple Gauge Boson Couplings	9
3	Diboson production at LHC	10
3.1	Proton-proton collisions	11
3.1.1	Hard Process	11
3.1.2	Parton Distribution Functions	11
3.1.3	Initial and Final State Radiation	12
3.1.4	Hadronization and the underlying event	12
3.2	Simulating effects of triple gauge boson couplings	12
3.2.1	Rewighting procedure	12
4	Data Analysis	13
4.1	ROOT, SFrame, CycleSequencer and AfterBurner	13
4.2	Event Selection	14
4.2.1	Background to WZ events	14
4.2.2	Datasets and Monte Carlo samples	15
4.2.3	Pileup reweighting	15
4.2.4	Preselection	15
4.3	Observables	18
4.3.1	Optimal Observables	19
5	Discussion	19
6	Conclusion	20
	Bibliography	21
A	Appendix	22
A.1	Information on the Monte Carlo samples used	22

1 Introduction

Particle physics is the study of the fundamental constituents of matter and the forces between them. However, which particles that have been considered fundamental has changed with time as new discoveries have been made. For the past 40 years, the Standard Model (SM) has successfully described nearly all phenomena observed at high energy collider experiments. However the Standard Model is expected to break down at a finite energy scale and as a result, much work is put in to look beyond the theory, an area called New Physics (NP). The search for New Physics is motivated by the desire to unravel the behavior of Nature and to really understand how the world works at the deepest possible level. The Large Hadron Collider (LHC) at CERN is currently the most powerful particle collider in the world and with the new upgrade finished in early 2015 and a new beam energy of up to 14 TeV, the prospects of discovering New Physics is looking very promising.

There are two ways to look for New Physics. A model-dependent search which considers predictions from a specific theory and a model-independent search which considers deviations from the Standard Model. This study will use a model-independent search, where the Standard Model is taken as a low energy approximation of new physics and can therefore be expanded in a similar way as a series expansion of a function in the neighborhood of a minimum. Specifically this project will look at possible deviations in the Electroweak theory of the Standard Model.

This project is a study of the charged triple gauge boson vertex WWZ and the associated triple gauge boson couplings. The vertex is included in the Standard Model and according the Standard Model, the couplings have a certain strength. If the couplings differ from the Standard Model, however, then the couplings are said to be anomalous and indicates new physics as an extension to the Standard Model. The effect of the anomalous couplings can be seen in the observables. In this study the effects of the anomalous triple gauge boson couplings will be investigated.

2 Theoretical Background

In this section we will present the theoretical background necessary for the understanding of the experimental search of this project. The modern theory of particle physics is called the Standard Model (SM) and it attempts to explain elementary particles in terms of their properties and interactions. Next a short review of quantum field theory (QFT), the framework on which the SM is built, is required along with a description of Lagrangian formalism and Feynman diagrams. Finally we will present the triple gauge boson vertices related to this study.

2.1 The Standard Model

The Standard Model (SM) of particle physics is the theory of how fundamental particles interact, governed by the four known fundamental forces. Listed by increasing strength, they are: gravitation, the weak nuclear, the electromagnetic and the strong nuclear force. All of the forces but gravity are understood in the context of quantum theory.

The fundamental particles can be divided into two groups: the fermions, also known as matter/anti-matter particles, and bosons. The bosons are further divided up into gauge bosons that act as force carriers and the newly discovered spin-0 Higgs boson, with the possibility of more Higgs bosons existing, though they have yet to be confirmed. The fermions are half-integer spin particles that are divided up into quarks and leptons. The quarks are positively charged and the leptons are negatively charged except for the neutral neutrinos. Of the negatively charged leptons we have the electron e , the heavier muon μ and tau τ . The light and neutral neutrinos consist of the electron neutrino ν_e , the muon neutrino ν_μ and the tau neutrino ν_τ .

Force	Relative strength	Theory	Mediator	Mass (GeV/c ²)	Range (m)
Strong	1	Chromodynamics	Gluons	0	10 ⁻¹⁵
Electromagnetic	10 ⁻³	Electrodynamics	Photon	0	Infinite
Weak	10 ⁻¹⁴	Electroweak theory	W [±] Z ⁰	80.385 91.1876	10 ⁻¹⁸
Gravitation	10 ⁻⁴³	General Relativity/ Geometrodynamics	Graviton	0	Infinite

Table 1: Here the strength is relative to the strong force. The numbers in this column should not be taken too literally as the strength of the forces depends on the nature of the source and how far away you are. What is listed in the theory part for gravitation is the relativistic theory of gravity. There is no quantum theory of gravity yet, though some have been proposed. For most purposes, the role of gravity is assumed to be negligible and nonsignificant in elementary particle physics.

Of the quarks, the most well known is the up and down quark of the first generation (see figure 1). Along with the eight gluons, the electrically neutral and massless mediators of the strong force, the quarks are the only particles with color charges and therefore the only interesting particles in the context of quantum chromodynamics (QCD). The mediator for the electromagnetic force is the neutral and massless photon and all electrically charged particles can interact within the theory of quantum electrodynamics (QED). For the weak force, the mediators are called *W* and *Z* bosons with masses about 80-90 times the mass of the proton. The two *W* bosons are electrically charged while the *Z* is neutral. All of the fermions are spin-1/2 and all of the observed gauge bosons are spin-1 [1].

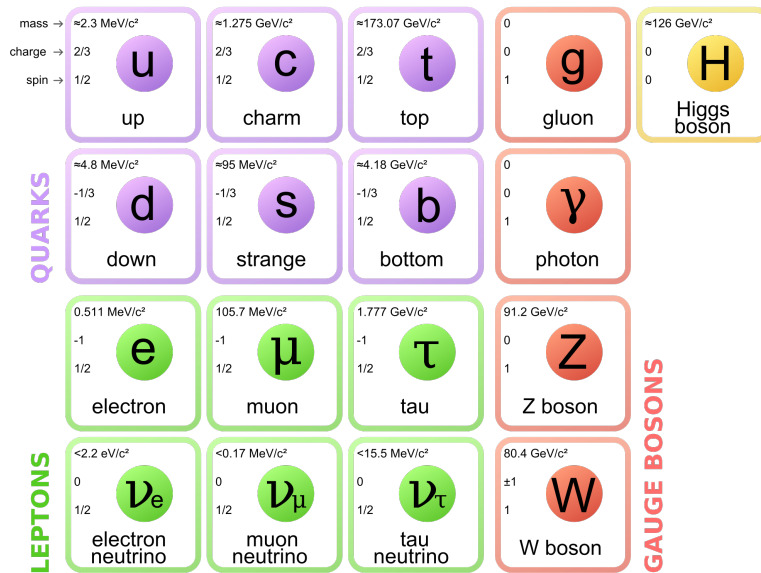


Figure 1: The particles of the Standard Model. The fundamental fermions are listed to the left in purple and green, and the bosons are to the right in red and yellow. Mass, charge and spin of all particles are included. Source: Wikimedia Commons.

All of the particles in the SM are assumed to be elementary, meaning they are treated as point particles, without internal structure or excited states. Another class of particles called hadrons is also observed in nature but they are composite particles consisting of either three quarks (baryons) or a quark and an

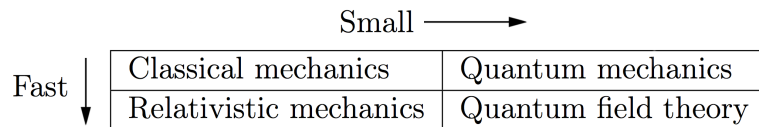
anti-quark (mesons). Due to color confinement, particles with color charge, that is quarks and gluons collectively known as partons, are not themselves directly observable, only their bound states.

For every particle, whether it is one of the elementary particles of the SM, or a hadron, there is an associated particle of the same mass, but opposite charge, called its antiparticle. In certain cases, for example with the neutral photon, the particle is its own antiparticle [2].

SM in its current state is not the final word on the subject, and the prospects of achieving higher energies in high energy experiments (the LHC achieved 8 TeV of energy before the long shutdown (LS1) in 2013 and will in 2015 when it reopens, run up to a planned energy of 14 TeV) opens up the possibility for discovering new physics (NP), physics beyond the SM.

2.2 Quantum Field Theory

Quantum Field Theory (QFT) is the theoretical framework on which elementary particle physics is built. As a complete review of quantum field theory would be beyond the scope of this project, this section on QFT will only serve as a short introduction. QFT can be seen as the unification of quantum mechanics and special relativity.



As elementary particles are extremely small¹ and typically also very fast (especially in the high energy experiments conducted at the LHC), elementary particle physics naturally falls under the dominion of QFT.

2.2.1 From classical physics to QFT and Lagrangian formalism

From the 18th century and onward, a refinement of the original Newtonian mechanics was developed by Lagrange and Hamilton among others. The formulation of QFT is built upon this formulation of classical mechanics so a quick summary is needed. In classical mechanics, the dynamics of the system can be described by two fundamental quantities, the Hamiltonian and the Lagrangian. The Lagrangian takes the form:

$$L = T - V \tag{1}$$

Where T denotes the kinetic energy and V is the potential energy of the system. From this we can define the action \mathcal{S} (also called the action integral), as the time integral over the Lagrangian L of the system:

$$\mathcal{S} = \int_{t_1}^{t_2} L(\mathbf{q}(t), \dot{\mathbf{q}}(t), t) dt \tag{2}$$

Here $\mathbf{q}(t)$ ² is the path taken by the system, moving from a configuration at time t_1 , the initial state, to the configuration at time t_2 , the final state. $\dot{\mathbf{q}}(t)$ is its derivative. The Principal of Least Action then states that the action \mathcal{S} of the system will take the smallest possible value, that is the variation of the action is equal to zero:

$$\delta\mathcal{S} = \delta \int_{t_1}^{t_2} L(\mathbf{q}(t), \dot{\mathbf{q}}(t), t) dt = 0 \tag{3}$$

¹It is unclear how small a fundamental particle like the electron actually is and whether it is even fundamental or if it does have a substructure. However, the size of it will be less than 10^{-18} m.

²Mathematical symbols in bold will denote a 3-dimensional vector in this project.

This is also called Hamilton's principle. This essentially means that an object should take the simplest and shortest path between two configurations [3].

2.2.2 The Feynman Path Integral

Next is to find a quantum formulation similar to the classical; a generalisation of the action principle in quantum theory. As we saw previously, classical mechanics can give a definite answer to the path of an object, but in quantum mechanics the path is not well-defined and we are rarely interested in the path of particle but rather the probability of finding a particle in particular state at a given time. This is also called the transition amplitude. In this case, we can write the Lagrangian as a spatial integral of a Lagrangian density \mathcal{L} :

$$L(\mathbf{q}(t), \dot{\mathbf{q}}(t), t) = \int \mathcal{L}(\phi, \partial_\mu \phi) d^3x \quad (4)$$

where ϕ and $\partial_\mu \phi$ are the fields and their corresponding derivatives. We can then write the action as:

$$\mathcal{S} = \int L dt = \int \mathcal{L}(\phi, \partial_\mu \phi) d^4x \quad (5)$$

And to continue with the analogy to the classical formulation, the variation of the action leads to the Euler-Lagrange equations of motion for the field $\phi(x)$:

$$\partial_\mu \left(\frac{\partial \mathcal{L}}{\partial(\partial_\mu \phi)} \right) - \frac{\partial \mathcal{L}}{\partial \phi} = 0 \quad (6)$$

So in QFT the situation is somewhat different from the classical picture as the system is allowed to follow all possible paths, not just the classical one, though in most cases the classical path is still dominating with smaller contributions from other paths. These contributions enter as quantum fluctuations around the classical path. In QFT then, instead of having a single uniquely defined path, we have a sum over all possible paths, or trajectories, which will be used to calculate a quantum transition amplitude. This sum is what we call the Feynman path integral. With a given Lagrangian and by the use of the Feynman path integral, the transition amplitudes (that is the probability of going from an initial state to a final state) are calculated using Feynman diagrams [4].

2.2.3 Feynman Rules and Diagrams

After writing up the Lagrangian for a system we then need to quantize it which can only be done by approximation. As described before we consider the classical path and then introduce quantum corrections with the method of Feynman diagrams. Feynman diagrams make it easy to distinguish between possible paths for the transition from a given initial state to a final state. For each different path you will have a topologically different Feynman diagram. Each diagram for a transition contributes to a sum called the amplitude or the matrix element \mathcal{M} , which contains all the dynamical information of the system. We calculate it by evaluating the relevant Feynman diagrams, using the Feynman rules appropriate to the interaction in question (i.e. electromagnetic, strong or weak). Feynman diagrams are basically built up of three building blocks as seen in figure 2, these are: vertices, propagators and loops, as described below.

Vertices: an interaction where a particle goes in and other particles go out. Given a certain type of interaction and the conservation laws, some vertices are allowed while others are not. Each vertex has a coupling constant which describes the strength at that vertex. These coupling constants are included in the calculation of the matrix element.

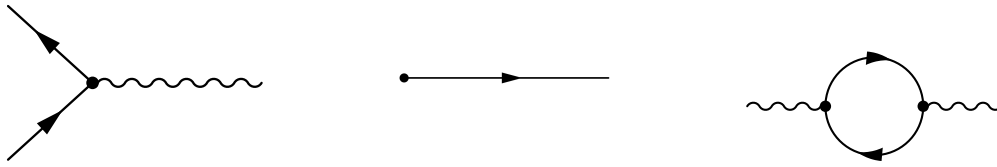


Figure 2: The three basic building blocks of Feynman diagrams. From left to right: vertex, propagator and loop.

Propagators: free movement between vertices. Corresponds to the momentum of the particle. Only external particles (particles that go in or out of a given diagram) are required to be 'on-shell', which means that the particle satisfy the equation: $E^2 - \mathbf{p}^2c^2 = m^2c^4$. Internal lines are also called virtual particles.

Internal loops: a particle/anti-particle pair created and annihilated in a loop.

The Feynman rules then determine how a certain building block contributes to the matrix element. The matrix element will be a function of the masses (m), the couplings (g) involved and the phase space information (Ω). For a more thorough description of Feynman rules at an introductory level, see reference [1].

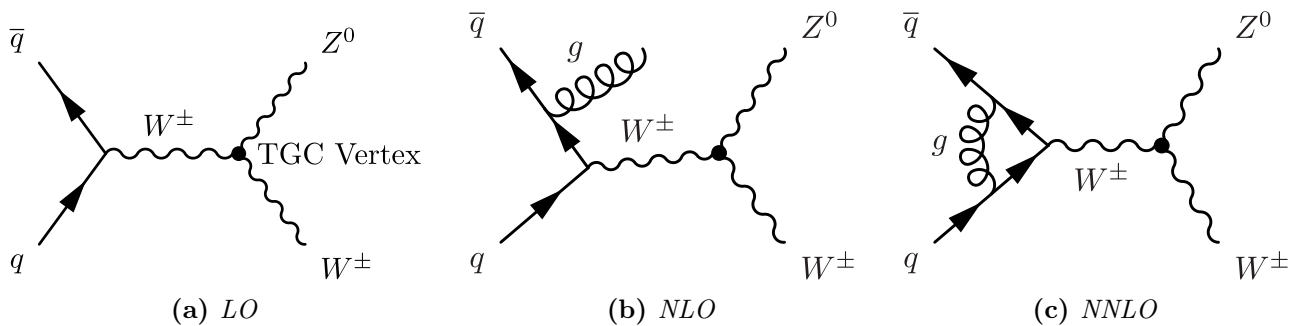


Figure 3: Feynman diagrams of WZ production at a hadron collider. (a) is the leading order diagram. (b) is the next-to-leading order diagram, with a gluon radiated by the quark. (c) is the next-to-next-to-leading order diagram, with a gluon loop. The diagrams are s -channel diagrams and contain a TGC vertex, as shown on (a).

In figure 3, a couple of different Feynman diagrams are shown. They all illustrate the same process: $q\bar{q} \rightarrow WZ$. Straight lines indicate fermions (leptons and quarks), while wiggly lines indicate photons, W and Z bosons. Lines that look like springs indicate gluons. The diagrams are meant to be read as if time flows horizontally, to the right. The arrows on the lines of the quark and anti-quark indicate whether it is a particle or an antiparticle. An arrow going 'backward in time' indicates an anti-particle. The simplest diagrams possible are called leading order (LO). With growing complexity we have next-to-leading order (NLO) and next-to-next-to-leading order (NNLO) diagrams. All of the diagrams contain a TGC vertex.

There exists three experimental probes of elementary particles interactions: bound states (described adequately by non-relativistic quantum mechanics), decays and scattering. For high energy experiments, scattering is the interesting one and the observable of choice is the differential scattering cross section:

$$d\sigma = \frac{|\mathcal{M}|^2}{\Phi} d\Omega \quad (7)$$

where ϕ is the incident flux and $d\Omega$ is the differential phase space element. The differential cross section will depend on the TGCs and will in fact be a quadratic function of the TGCs. The calculation of the scattering cross section is called Fermi's Golden Rule for Scattering [1].

2.2.4 Renormalization

The method of Feynman diagrams works very well as long as the diagrams in question do not contain any loops. If loops are present, it is possible for the scattering amplitude to diverge due to the unconstrained momentum of the particles in the loop. This will lead to unphysical results as all observable quantities must be finite. Historically, this disaster held up the development of quantum electrodynamics and QFT in general for nearly two decades until systematic methods were developed for coping with this problem and this method is now called renormalization. It is essentially a 'sweeping under the rug' solution. To get around the divergences, a cutoff scale Λ on the high-momentum phase-space is introduced to cancel the terms going to infinity by letting $\Lambda \rightarrow \infty$. If infinities arising from higher-order diagrams (with loops) can be accommodated by renormalization we say that we have a renormalizable theory. Having a renormalizable theory with a certain cutoff scale Λ , means that the scattering amplitudes will be a function of this cutoff scale as well as the masses, coupling constants and phase space information:

$$\mathcal{M} = \mathcal{M}(m, g, \Omega, \Lambda) \tag{8}$$

At this point all the divergent, Λ dependent terms appear in the final answer in the form of additions to the masses and coupling constants. If taken seriously, this means that the physical masses and couplings are not the m 's and g 's that appeared in the original Feynman rules, but rather the renormalized ones:

$$m_{\text{physical}} = m + \delta m, \quad g_{\text{physical}} = g + \delta g \tag{9}$$

The fact that these extra factors are infinite is disturbing but not catastrophic for the theory as we never measure them in experiments. What we measure is the physical values, which are finite. Evidently then the factors m and g must contain compensating infinities [1].

2.2.5 Symmetries

Symmetries are a recurring theme in physics and play an important role in elementary particle physics. This is in part because of their relation to conservation laws and in part because they permit one to make some progress when a complete dynamical theory is not yet available. A famous theorem that relates symmetries and conservation laws is Noether's theorem which states that every symmetry of nature yields a conservation law and conversely, every conservation law reflects an underlying symmetry. By symmetry we mean an operation you can perform (at least conceptually) on a system that leaves it invariant, that is it carries into a configuration that is indistinguishable from the original one. To construct the Lagrangian, we impose the two following symmetries:

Lorentz invariance: required as the velocity of the particles reach relativistic limits. A system is said to be Lorentz invariant if it remains the same under the Lorentz transformation.

Gauge invariance: fundamental requirement from which the nature of particle interactions is deduced. For gauge theories, invariance is required under the gauge transformation.

A possible Lagrangian would in classical mechanics take the form of equation 1. In QFT we can give a similar Lagrangian with a complex scalar field:

$$\mathcal{L} = \partial_\mu \phi^\dagger \partial^\mu \phi - V(\phi^\dagger \phi) \tag{10}$$

This Lagrangian has a global symmetry as it is invariant under the gauge transformation $\phi(x) \rightarrow \phi'(x) = e^{i\alpha(x)}\phi(x)$, which is dependent on space-time. From electrodynamics we have the Maxwell equations on the form:

$$\mathbf{E} = -\nabla\phi - \frac{\partial\mathbf{A}}{\partial t}, \quad \mathbf{B} = \nabla \times \mathbf{A} \quad (11)$$

which are invariant under the local gauge transformation:

$$\mathbf{A}' = \mathbf{A} + \nabla\lambda, \quad \phi' = \phi - \frac{\partial\lambda}{\partial t} \quad (12)$$

Which is a function of the space-time coordinates and therefore differs from the global transformation. Furthermore there are three discrete symmetries:

Charge conjugation, C: changes particles to their anti-particles and the other way around, $\mathbf{C}\psi = \bar{\psi}$.

Parity transformation, P: reverses the space coordinates $(\bar{x}, t) \rightarrow (-\bar{x}, t)$.

Time-reversal transformation, T: reverses the time coordinate $(\bar{x}, t) \rightarrow (\bar{x}, -t)$.

Any relativistic field theory must be invariant under CPT transformations, but not necessarily under C , P and T , separately. Experiments show that gravity, strong- and electromagnetic interaction are symmetric under C , P and T transformations while weak interaction violate C , P and CP .

2.2.6 Quantum Electrodynamics

Quantum electrodynamics (QED) is the oldest, simplest and arguably the most successful of the dynamical gauge quantum field theories, and the other theories are modelled on it. It describes the interaction between charged particles (electrons, electron-like particles and quarks) and photons. All electromagnetic phenomena are ultimately reducible to the following elementary process:

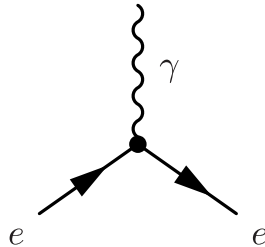


Figure 4: A simple QED process. This is not a valid Feynman diagram in itself but the simplest building block of one in QED. Here e indicates any charged fermion and not necessarily an electron.

While particles are described by the Schrödinger's equation in non-relativistic quantum mechanics, spin-1/2 particles are, in relativistic quantum mechanics, described by the Dirac equation:

$$\begin{aligned} i\hbar\gamma^\mu\partial_\mu\psi - mc\psi &= 0 \\ (i\gamma^\mu\partial_\mu - mc)\psi(x) &= 0 \quad (\text{Natural units: } \hbar = c = 1) \end{aligned} \quad (13)$$

which naturally makes it the starting point of QED, as leptons are spin-1/2³. The kinematic and dynamics of the particle field $\psi(x)$ are captured in the Lorentz invariant Dirac Lagrangian:

$$\mathcal{L}_{\text{Dirac}} = \bar{\psi}(x)(i\gamma^\mu\partial_\mu - m)\psi(x) \quad (14)$$

³As a side note, particles of spin 0 are described by the Klein-Gordin equation and particles of spin 1 by the Proca equation. The derivation of these three equations is beyond the scope of this study.

which is the Lagrangian describing the dynamics of the free Dirac fermions. Here ψ is a spinor (an element of complex vector space) and not a scalar like ϕ . This is due to the fact that electrons, which are the particle of interest here, have a spin with a direction that cannot be described by a scalar field. The Lagrangian can be made invariant by introducing a four-vector $A^\mu(x) = (\phi, \mathbf{A})$ with the transformation:

$$A_\mu(x) \rightarrow A'_\mu(x) \equiv A_\mu(x) - \frac{1}{e}\partial_\mu\alpha(x) \quad (15)$$

where e is the coupling constant between the particle and the introduced gauge field. The ordinary derivatives have to be replaced with the covariant derivative:

$$\partial_\mu \rightarrow D_\mu \equiv \partial_\mu - ieA_\mu \quad (16)$$

$$D_\mu\psi(x) \equiv (\partial_\mu - ieA_\mu(x))\psi(x) \quad (17)$$

With these substitutions the Lagrangian is then given by:

$$\mathcal{L} = \bar{\psi}(x)(i\gamma^\mu\partial_\mu - m)\psi(x) - e\bar{\psi}(x)\gamma^\mu\psi(x)A_\mu(x) \quad (18)$$

which is invariant under local transformation. The field A_μ does not have any degrees of freedom and therefore cannot propagate in space-time. The property to propagate can be given by introducing an additional kinematic term in the Lagrangian:

$$\mathcal{L}_{\text{kinematic}} = -\frac{1}{4}F^{\mu\nu}F_{\mu\nu} \quad (19)$$

where we have that $F = \partial_\mu A_\nu - \partial_\nu A_\mu$. This makes it possible to identify the field A_μ as the photon field and it is now equivalent with the kinematic term from classical electrodynamics $\mathcal{L}_{kin} = \frac{1}{2}(\mathbf{E}^2 - \mathbf{B}^2)$. The mass of the photon would be given by a mass term for the gauge field $\mathcal{L}_{mass} = \frac{1}{2}m^2 A^\mu A_\mu$ but this would violate gauge invariance, requiring that the photon must be massless. This then makes it possible to write the Lagrangian for spin-1/2 particles interacting with a massless electromagnetic field (propagated by photons):

$$\mathcal{L}_{QED} = \bar{\psi}(x)(i\gamma^\mu D_\mu - m)\psi(x) - \frac{1}{4}F^{\mu\nu}F_{\mu\nu} \quad (20)$$

As mentioned in the beginning of this subsection, the weak and strong quantum field theories, called Quantum Flavor Dynamics (QFD)⁴ and Quantum Chromodynamics (QCD), are modelled on the formulation of QED. The structure of these theories are however much richer and a derivation of them would be too big of a mouthful so we simply state the results of the electroweak theory, which is the important interaction for this project.

2.2.7 Electroweak theory

The electroweak theory (EW theory), also known as the Glashow-Salam-Weinberg (GWS) theory, is the unification of the electromagnetic interaction and the weak interaction. It consists of four gauge fields: the photon-, the W^\pm and the Z^0 field. These are collected under the gauge symmetry $SU(2)\times U(1)$. The gauge transformation actually requires the masses of the bosons of the weak interaction to be massless like the photon which is in disagreement with results from experiments that show that they are in fact quite massive, see table 1 for masses. However this is fixed as the $SU(2)\times U(1)$ symmetry is spontaneously broken by the Higgs mechanism which is the cause of the large mass of the W^\pm and

⁴Albeit the weak interaction is better understood in the context of the electroweak theory.

Z^0 bosons. Before the symmetry breaking, the theory contains four massless gauge bosons. One for $U(1)$, \mathcal{B}_μ and three for $SU(2)$, \mathcal{W}_μ^i , where $i = 1, 2, 3$. The gauge boson field strength is then:

$$\mathcal{L}_g = -\frac{1}{4}\mathcal{W}_{\mu\nu}^i\mathcal{W}_i^{\mu\nu} - \frac{1}{4}\mathcal{B}_{\mu\nu}\mathcal{B}^{\mu\nu} \quad (21)$$

The field strength tensors of the four fields are given by:

$$\mathcal{B}_{\mu\nu} = \partial_\mu\mathcal{B}_\nu - \partial_\nu\mathcal{B}_\mu \quad (22)$$

$$\mathcal{W}_{\mu\nu}^i = \partial_\mu\mathcal{W}_\nu^i - \partial_\nu\mathcal{W}_\mu^i - g\varepsilon_{ijk}\mathcal{W}_\mu^j\mathcal{W}_\nu^k \quad (23)$$

The two terms of equation 21 are the kinetic energy and the self-coupling of the \mathcal{W}_μ^i fields and the kinetic energy of the \mathcal{B}_μ . The field strength tensors of $SU(2)$ (of equation 23) contain a bilinear term, and the term generates the trilinear and quadrilinear self-couplings of the $\mathcal{W}_{\mu\nu}^i$. This corresponds to the self-couplings of the bosons. The self-interaction is a consequence of the necessity to maintain gauge invariance. Not all interactions are allowed though. There are many interesting aspects of the electroweak theory but the one we are interested in is the interaction between the gauge bosons themselves.

2.3 Anomalous Triple Gauge Boson Couplings

On the basis of the standard model and quantum field theory we have the basic knowledge to introduce triple gauge boson couplings and their vertices where the three gauge-bosons interact. A very interesting result of the electroweak theory is that interactions between the gauge bosons themselves are allowed. This leads to three and four boson vertices. In this project we are interested in interactions with three gauge bosons. This is possible as the W^\pm bosons carry charge. Because of this, interactions like ZZZ and ZZy are not possible and similar vertices including an odd number of W^\pm bosons, such as WZZ and WZy are not possible either, due to charge conservation. The only possible TGCs are WWy and WWZ , with the latter being the interaction we will be concerned with.

This project will look at the WWZ vertex through the introduction of anomalous triple gauge couplings (aTGCs) by the method of effective Lagrangian. A coupling is anomalous if it is not present in the SM Lagrangian, whereas the entire vertex is called anomalous if it is not found in the SM. As mentioned before equation 21 allows both cubic and quartic self-coupling terms for the gauge bosons of the electroweak theory. In the SM the Lagrangian for the WWZ interaction takes the form:

$$\mathcal{L}_{SM}^{WWZ} = -ig_{WWZ} [(1 + \Delta g_1^Z)Z^\mu(W_{\mu\nu}^-W^{+\nu} - W_{\mu\nu}^+W^{-\nu}) + (1 + \Delta\kappa_Z)W_\mu^+W_\nu^-Z^{\mu\nu}] \quad (24)$$

The Lagrangian only includes operators with mass-dimension 4, which is a requirement for renormalizability. To study the anomalous couplings we must introduce an effective theory which is a low energy approximation. Writing an effective Lagrangian is a smart way to introduce New Physics (NP) to an existing model. The concept is similar to the series expansion of a mathematical function, where the expansion only includes a couple of terms but is a good enough approximation in the neighborhood of a certain point. The effective Lagrangian will assume that the scale of the new physics, Λ , will be much higher than the scale of the SM, as otherwise we would have seen the contributions of these terms already. Another assumption is that the expansion will break down when the energy approach that of Λ . We can then write a corresponding effective Lagrangian for low energies in powers of the low energy fields, l_I , and their derivatives:

$$\mathcal{L}_{eff} = \sum_I c_I \mathcal{O}_I(l_I) \quad (25)$$

where \mathcal{O}_I is the effective interactions with mass dimension d_I . c_I is the effective coupling which depends on the mass scale of the heavy degrees of freedom, Λ and the d_I in the way $c_I \propto \Lambda^{4-d_I}$. A complete derivation of the effective Lagrangian is out of scope for this project, so we will simply present it as it is commonly written in the literature (see for example reference [5]).

The Lagrangian for the WWZ vertex is then:

$$\begin{aligned}
 \mathcal{L}_{eff}^{WWZ} = & -ig_{WWZ}[(1 + \Delta g_1^Z)Z^\mu(W_{\mu\nu}^-W^{+\nu} - W_{\mu\nu}^+W^{-\nu}) \\
 & + (1 + \Delta\kappa_Z)W_\mu^+W_\nu^-Z^{\mu\nu} + \frac{\lambda_Z}{m_W^2}Z^{\mu\nu}W_\nu^{+\rho}W_{\rho\mu}^- \\
 & + ig_5^Z\varepsilon_{\mu\nu\rho\sigma}((\partial^\rho W^{-\mu})W^{+\nu} - W^{-\mu}\partial_\rho W^{+\nu})Z^\sigma \\
 & + ig_4^Z W_\mu^-W_\nu^+(\partial^\mu Z^\nu + \partial^\nu Z^\mu) \\
 & + \frac{\tilde{\kappa}_Z}{2}W_\mu^-W_\nu^+\varepsilon^{\mu\nu\rho\sigma}Z_{\rho\sigma} - \frac{\tilde{\lambda}_Z}{2M_W^2}W_{\rho\mu}^-W_\nu^{+\mu}\varepsilon^{\nu\rho\alpha\beta}Z_{\alpha\beta}]
 \end{aligned} \tag{26}$$

where $W_{\mu\nu}^- = \partial_\mu W_\nu^- - \partial_\nu W_\mu^-$, $Z_{\mu\nu} = \partial_\mu Z_\nu - \partial_\nu Z_\mu$. From the effective Lagrangian we find 7 coupling parameters for the WWZ vertex⁵. The coupling parameters are dimensionless and setting them to zero will give us the SM as before. The convention here is

$$\Delta g_1^Z = g_1^Z - 1, \quad \Delta\kappa_Z = \kappa_Z - 1 \tag{27}$$

as the intention is to describe deviations from the SM. Because of this the derived quantities are used. The 7 coupling parameters are: Δg_1^Z , $\Delta\kappa_Z$, λ_Z , g_5^Z , g_4^Z , $\tilde{\kappa}_Z$ and $\tilde{\lambda}_Z$. As the Lagrangian has dimension $(mass)^4$, the operators associated with the couplings will either have dimension $(mass)^4$ or $(mass)^6$. We notice that the dimensionality of the operators associated with the 7 coupling parameters are:

Mass dimension 4: g_1^Z , g_4^Z , κ_Z and $\tilde{\kappa}_Z$.

Mass dimension 6: g_5^Z , λ_Z and $\tilde{\lambda}_Z$.

This is important to note when comparing the terms as higher dimension operators have higher energy dependence, which makes them more dominant than the others. An interesting thing to also note is the CP-behavior of the coupling parameters. The three couplings Δg_1^Z , $\Delta\kappa_Z$ and λ_Z are CP-conserving while g_5^Z is CP-conserving but C/P-violating. The rest, g_4^Z , $\tilde{\kappa}_Z$ and $\tilde{\lambda}_Z$, are CP-violating. The coefficients we will concern us with are the three CP-conserving coefficients Δg_1^Z , $\Delta\kappa_Z$ and λ_Z .

3 Diboson production at LHC

In this section we will present the phenomenology, that is the interface between the theory and the experiment, of this study. Specifically it will be the phenomenology of hadron colliders. This section is necessary as there is still a long way from the effective Lagrangian introduced in the previous section, to the final states observed in the detector. Experimental particle physicists use so-called Monte Carlo event generators in order to make precise predictions about kinematics distributions. An event generator is an application that, given a scattering amplitude \mathcal{M} for a hard process and a parton distribution function (pdf), can compute the final states predicted by the theory. This is often referred to as the *truth*-level. A typical Monte Carlo event generator technique for producing an event sample, is the *hit-and-miss* technique, which allows for a random event selection according to the differential cross sections (event weights). Some Monte Carlo event generators include POWHEG, PYTHIA, BHO,

⁵There are 7 coupling parameters for the $WW\gamma$ vertex as well, making it 14 in total for the anomalous TGCs. The effective Lagrangian can be written in a similar way for the $WW\gamma$ or generalised for the WWV vertex, with $V = \{Z, \gamma\}$.

Sherpa, MC@NLO and Jimmy. A simulation of the detector is also necessary. This is done with the high-energy detector simulation Geant4. Finally the event needs to be reconstructed. This is done for both data and simulation. This makes it possible to begin an analysis of the signal of interest, after removing any fake signal from other processes which is referred to as 'background'.

3.1 Proton-proton collisions

A high energy proton-proton collision event can be thought of in this (slightly simplified) time-order:

1. Two protons come adequately close to each other. Each proton is characterized by a parton distribution function (see section 3.1.2).
2. One ingoing parton (quark or gluon) from each proton beam enters the hard process. It is possible for the partons to radiate photons and gluons in what is called 'initial state radiation'.
3. The hard process produces a number of outgoing particles. These particles may radiate final state radiation.
4. Unstable particles are decayed. Hadronization happens for particles with color charge.
5. Some semi-hard process may happen between the other partons of the two protons.
6. The remnants of the proton may have some structure and color charge and can interact with the other particles of the final state.

The event generator will simulate all of these steps. In the following subsections these items will be explained a little more in depth [5].

3.1.1 Hard Process

The hard process is the key process of the Monte Carlo event generator. A hard QCD process is a process for QCD jet production over a minimum transverse momentum p_T threshold. The hard process will produce quarks and gluons (collectively known as partons) with a very high transverse momentum, p_T . The hard process of interest in this project, is the production of a WZ system from quarks, that is the process $q\bar{q} \rightarrow WZ$ as illustrated in figure 3(a). The differential cross section for this process is written (as we saw in equation 7):

$$d\sigma(q\bar{q} \rightarrow WZ) = \frac{1}{2\hat{s}} |\mathcal{M}(q\bar{q} \rightarrow WZ)|^2 \frac{d\cos(\theta)d\sigma}{8(2\pi)^2} \quad (28)$$

where ϕ and θ are the azimuthal and polar angles, constituting the phase space. The differential cross section is often referred to as the *event weight*.

3.1.2 Parton Distribution Functions

A parton distribution function (pdf) is used to model the compositeness of the proton. The pdf expresses the probability for a quark or gluon (collectively called partons) to have a certain momentum fraction x of the total energy of the proton. The pdf will give the probability as a function of momentum fraction of the i 'th parton, x_i , and the momentum transfer scale Q of the collision, written as $f(x_i, Q^2)$. The energy scale in this case, for WZ production, is the electroweak energy scale which is a lot larger than the strong (QCD) scale.

3.1.3 Initial and Final State Radiation

The incoming and outgoing partons of the hard process may radiate photons and gluons before and after the process has happened. This is depicted in figure 3(b) represented by a next-to-leading order (NLO) Feynman diagram as this is actually a higher order correction. A full NLO treatment can be very CPU intensive but it has been recently made possible to calculate full NLO differential cross sections using event generators. MC@NLO is an example of an event generator with such a capability.

3.1.4 Hadronization and the underlying event

The partons involved in the hard process can only be regarded as free particles on the timescales of the QCD hard process. This means that they are organized into colorless hadrons so that they may obey color confinement. This is approached by models (such as the Lund string model or the cluster model) and is incorporated into the event generators.

The underlying event is everything that is not related to the interaction of the hard process. This refers primarily to interactions between the remnants of the protons. Furthermore, the partons can undergo interactions scattering with other partons and give multiple interactions.

3.2 Simulating effects of triple gauge boson couplings

As outlined in section 2.3, the effect of the anomalous TGCs can be included as extra terms in the effective Lagrangian. The effects of the anomalous TGCs will be included by a reweighting procedure. The reweighting routine will take the SM cross section of the WZ event and rescale it to include the anomalous contributions. The rescaling is done using the entire sample of SM WZ events and is therefore much faster than using a MC event generator that includes every effect of the anomalous couplings.

3.2.1 Reweighting procedure

Given a sample of Monte Carlo events generated at the SM and without TGCs, then the events can be reweighted to non-SM TGC values by applying an event specific weight to each event:

$$w = \frac{d\sigma_{TGC}}{d\sigma_{SM}} \quad (29)$$

The differential cross section $d\sigma_{TGC}$ can be calculated for an event, given values of the TGCs and the full matrix elements \mathcal{M} . The effects of the anomalous TGCs included in the Lagrangian (equation 26) will be added to the cross section of the process by the matrix element. As the TGCs are added linearly to the Lagrangian and the differential cross sections dependence of the matrix element, $d\sigma \propto |\mathcal{M}|^2$, the effects of the anomalous couplings will take the form of a quadratic equation:

$$d\sigma = F_0 + a \cdot F_1 + a^2 \cdot F_2 \quad (30)$$

with $F_0 = d\sigma_{SM}$. Having only one coupling will give three independent equations so the coupling a will take the values $a = \{0, 1, -1\}$. This will give us the system:

$$\begin{aligned} d\sigma_1 &= F_0 \\ d\sigma_2 &= F_0 + F_1 + F_2 \\ d\sigma_3 &= F_0 - F_1 + F_2 \end{aligned} \quad (31)$$

or on matrix form:

$$\begin{pmatrix} d\sigma_1 \\ d\sigma_2 \\ d\sigma_3 \end{pmatrix} = \begin{bmatrix} 1 & 0 & 0 \\ 1 & 1 & 1 \\ 1 & -1 & 1 \end{bmatrix} \begin{pmatrix} F_0 \\ F_1 \\ F_2 \end{pmatrix} \quad (32)$$

and in a more compact form: $d\sigma = \hat{A} \cdot \mathbf{F}$. We can then obtain the coefficients given the differential cross sections and the values of the coupling constants. Isolating \mathbf{F} gives us:

$$\mathbf{F} = \hat{A}^{-1} d\sigma \quad (33)$$

The matrix \hat{A} is invertible as the system of equations in equation 31 and 32 are linearly independent. This notation can be used to incorporate more than one coupling (in our case that would be three). For three couplings, α_1 , α_2 and α_3 , we have:

$$\begin{aligned} d\sigma_{TGC} &= (1 \quad \alpha_1 \quad \alpha_2 \quad \alpha_3) \begin{bmatrix} F_0 & F_1 & F_2 & F_3 \\ 0 & F_4 & F_5 & F_6 \\ 0 & 0 & F_7 & F_8 \\ 0 & 0 & 0 & F_9 \end{bmatrix} \begin{pmatrix} 1 \\ \alpha_1 \\ \alpha_2 \\ \alpha_3 \end{pmatrix} \\ &= F_0 + \alpha_1 F_1 + \alpha_2 F_2 + \alpha_3 F_3 + \alpha_1^2 F_4 + \alpha_1 \alpha_2 F_5 \\ &\quad + \alpha_1 \alpha_3 F_6 + \alpha_2^2 F_7 + \alpha_2 \alpha_3 F_8 + \alpha_3^2 F_9 \end{aligned} \quad (34)$$

Note that $d\sigma_{SM} = F_0$. This can be further generalised to n couplings. Here the \hat{F} matrix is 4×4 matrix on upper triangular form. A program following the reweighting procedure will calculate all the coefficients F for every event. Then the weights from equation 29 can be calculated. For the SM the event weight will of course be $\frac{d\sigma_{SM}}{d\sigma_{SM}} = 1$.

Calculating the weight after the event generator step is usually referred to as the *afterburner* method. The alternative would be to calculate the weight during the event generation. The two methods are fundamentally the same though the afterburner method provides greater flexibility but also added complexity, as the calculation of the weights and the event generation are decoupled and therefore allow for modification. The afterburner method allows for using whatever event generator as the generation of weight is no longer needed by the event generator. In addition, new processes can be considered by adding a new matrix element to the generator [5].

4 Data Analysis

With the theoretical background for the anomalous triple gauge-boson couplings established and the phenomenology for the diboson production at LHC, we can then turn to examine how these couplings can be observed in experiments and which observables are sensitive to the anomalous TGCs. In this section we will describe the event selection and preselection cuts. Then we will go over the analysis methods used for extracting the anomalous TGCs.

4.1 ROOT, SFrame, CycleSequencer and AfterBurner

For its data analysis, this project used the programming library **ROOT**, developed at CERN. ROOT is a cross-platform, object-oriented library as well as a collection of command-line and GUI applications, written in C++. For more information on ROOT, see reference [6] and [7].

SFrame is a C++ framework built around the ROOT libraries for analysing particle physics data. It reads ROOT files and adds support for creating ROOT objects (histograms, ntuples, etc.) and can be configured through XML files. SFrame makes it possible to run ROOT code in parallel.

CycleSequencer is an application written on top of SFrame, by the two PhD students, Ask Emil Løvschall-Jensen and Kristian Gregersen at the Niels Bohr Institute, under the supervision of Jørgen Beck Hansen. CycleSequencer makes it possible to process ATLAS data and Monte Carlo files (samples) through the use of *selectors* and *tools*. CycleSequencer is, roughly speaking, divided up into three states: (1) initialization - where all variables and classes are declared, (2) Execution - where every event (proton-proton collision) is read in one by one, (3) Finalization - where the output is saved and histograms are plotted and so on. The *selectors* are C++ files used, for example, to select electrons or photons in an event that you want to save. This makes it possible to discard events from the data files that are not of interest for the project. This is called event selection or event cuts. This greatly reduces the file sizes of the datasets/MC samples (by more than 99%). The *tools* are, for example, to do Pileup reweighting.

AfterBurner is a standalone program, written partly in C++ and partly in Fortran, using the ROOT library. It calculates the differential cross sections needed for the method of Optimal Observables (OO). It takes as input a ROOT file, calculates the matrix elements for F (as outlined in the section 3.2) and saves them in an output ROOT file. The coefficients determined will be for the three parameters, Δg_1^Z , $\Delta \kappa_Z$ and λ_Z , from the effective Lagrangian from section 2.3.

4.2 Event Selection

The event selection is a way to extract the signal from the background, or in other words, to separate the final states originating from the process that is of interest from the the final states originating from other processes which produce a similar looking final state. As the signal is usually quite small and the background is quite large, the selection of the events of interest and the rejection of the background events has to be optimised. For this project the process of interest is the $pp \rightarrow WZ$ (Feynman diagram shown in figure 3(a)) where the final states considered contains three leptons and a neutrino, as the W decays into a lepton and a neutrino and the Z decays into two leptons. The goal of the event selection is to remove as much as possible of the background associated with the final state of interest (three leptons and one neutrino) while leaving as much of the signal as possible, so we in the end have a clear signal to work on. A cut based event selection is used to ensure (1) only well defined leptons and (2) that reconstruction of W and Z is possible [5].

4.2.1 Background to WZ events

The final states of three leptons and one neutrino are considered very pure but it is still not straightforward to select the events of interest as other processes could have an experimental signature that resemble that of the signal. There are some physics processes that are of special concern during the selection and are considered important background contributions. These are the most significant background processes in the search for WZ events:

Backgrounds with four leptons from the hard process. A ZZ with leptonic decay (four leptons) can imitate the WZ signature if one of the leptons fails to be detected. The process $ZZ \rightarrow 4l$ is sensitive to the neutral TGCs, which are another type of TGC than the one focused on in this project. This is an important background process, as it closely resembles the WZ process.

Backgrounds with two leptons from the hard process. A Z produced with a jet can be misidentified as a WZ event if the jet is misidentified as a lepton. The process $t\bar{t} \rightarrow WbW\bar{b}$ can be misinterpreted if one of the jets is misidentified as a lepton with the W 's decaying to two leptons and two neutrinos. A process with WW final state could also be misinterpreted if a third lepton came from the initial- or final state radiation.

Backgrounds with one lepton from the hard process. A W produced with jets can be misidentified if two of the jets are falsely detected as leptons.

Backgrounds with no leptons from the hard process. Dijets are part of the large background from QCD.

4.2.2 Datasets and Monte Carlo samples

The data set selected for analysis in the project is taken with the ATLAS detector at LHC in 2012 at $\sqrt{s} = 8$ TeV and an integrated luminosity of $\int \mathcal{L} dt = 20.28 \text{ fb}^{-1}$.

The Monte Carlo samples of WZ events used for comparison with data and to test the event selection, are officially produced ATLAS Monte Carlo samples. There are two sets of MC samples. A set of Standard Model WZ events generated using the Sherpa event generator [8] and another set with WZ simulated to include TGCs generated using the MC@NLO event generator [9]. Both sets are for 2012 at $\sqrt{s} = 8$ TeV. Sets of MC samples for the backgrounds of ZZ , $t\bar{t}$, $Z + jets$ and WW are also used as described before. MC samples with the backgrounds $W + jets$ and Dijets were not used.

Both the data files and the MC files are ROOT files in the Derived Physics Data Detail-3 (D3PD) data format, a standard ROOT tree data structure, widely used by physics groups in the ATLAS collaboration. The data format allows for fast computation times and provides information on electrons, muons, taus, jets, missing transverse energy \cancel{E}_T , track parameters and truth (if the D3PD file contains simulated events). A standard set of variables is saved in a tree called "physics" within the D3PD file, where each entry in the tree corresponds to one selected event.

4.2.3 Pileup reweighting

There may be a discrepancy between the event pileup (multiple proton-proton collisions in a collision of one bunch) of the Monte Carlo samples and that of the data samples. This happens if the event pileup has not been simulated correctly in the event generation. This discrepancy must be accounted for and this is done with pileup reweighting. The reweighting of Monte Carlo samples to the pileup conditions of the data samples is done with the ATLAS tool for pileup reweighting. This is one of the tools used with the program CycleSequencer.

4.2.4 Preselection

The event preselection ensures at first that the detector is in a condition so that the event is sensible and that the event itself fulfills some set minimum requirements so it is fit for further investigation. These are:

Good-Runs-List. The first requirement is that the event is in a so-called Good-Runs-List (GRL); a run list prepared by the ATLAS data quality group. If the event is in the GRL it is deemed valid for analysis. The GRL is one of the tools used by CycleSequencer.

ATLAS Liquid Argon (LAr) calorimeter error. The Liquid Argon (LAr) sampling calorimeter is a key detector component in the ATLAS experiment and during a larger part of the time taking data, the LAr calorimeter was affected by a failure. This resulted in the need to cut out events within the affected region of measurements.

Number of tracks at primary vertex. The primary vertex must have at least two reconstructed tracks associated with it. By primary vertex we mean the reconstructed vertex with the highest track multiplicity.

The second part of the preselection process happens when the event passes the first part. Here the physical objects are subjected to a series of cuts. Both electrons and muons must originate from the primary vertex. The missing transverse energy \cancel{E}_T used in project is `MET_RefFinal`, and here it is required that $\cancel{E}_T > 20$ GeV. For all leptons we require that:

$$\Delta R = \sqrt{\Delta\eta^2 + \Delta\phi^2} < 0.2 \quad (36)$$

which is a derived quantity for describing a 2-dimensional radial distance between two points in the detector. The preselection criteria for the physical objects are:

Muons. The reconstructed muons are required to have $|\eta| < 2.4$ and $p_T > 20$ GeV.

Electrons. The reconstructed electrons are required to have $|\eta| < 2.47$ and $p_T > 20$ GeV.

Neutrinos. The neutrino in the final state from the W is not directly observable, but is seen indirectly through missing transverse energy \cancel{E}_T . For this study we have assumed that the transverse energy of the neutrino is the same as the missing transverse energy ($E_{\nu T} = \cancel{E}_T$) hence ignoring other effects that may contribute to the missing energy. If the criteria $\cancel{E}_T > 20$ GeV is fulfilled, we determine the z component of the neutrinos four-momentum, $p_{\nu z}$. This is done by solving the second order polynomial:

$$(k_2^2 - k_1^2)p_{\nu z}^2 + 2k_3k_2p_{\nu z} - (k_1^2E_{\nu T}^2 + k_3^2) = 0 \quad (37)$$

with

$$k_1 = 2E_\mu, \quad k_2 = 2p_{\mu z}, \quad k_3 = M_W^2 - m_\mu^2 + 2p_{\mu T}p_{\nu T} \quad (38)$$

and where $p_{\nu z}$ is the only unknown quantity. This polynomial is solvable and will give two, one or zero real solutions. For one solution the choice is easy. For zero solutions, we set the discriminant to zero, solve for M_W and update k_3 to include this new value and we will be able to find one real solution. For two solutions it would be correct to use both solutions and weight them 1/2 so we are unbiased. For this study however we have done the same as for the zero solution case and in all cases will have just one solution for $p_{\nu z}$. For a more thorough description of this calculation, see ref. [4].

Before being able to form the WZ pair, the event must fulfill some reconstruction requirements for each boson:

Z reconstruction. A pair of leptons that are candidates for being identified as the decay products of a Z boson, needs to satisfy the following requirements: (1) they must have opposite electric charge, (2) they must have the same flavor and (3) their combined invariant mass must be compatible with the mass of the Z , i.e. lie within a range of ± 20 GeV of the Z mass ($m_Z = 91.1876$ GeV).

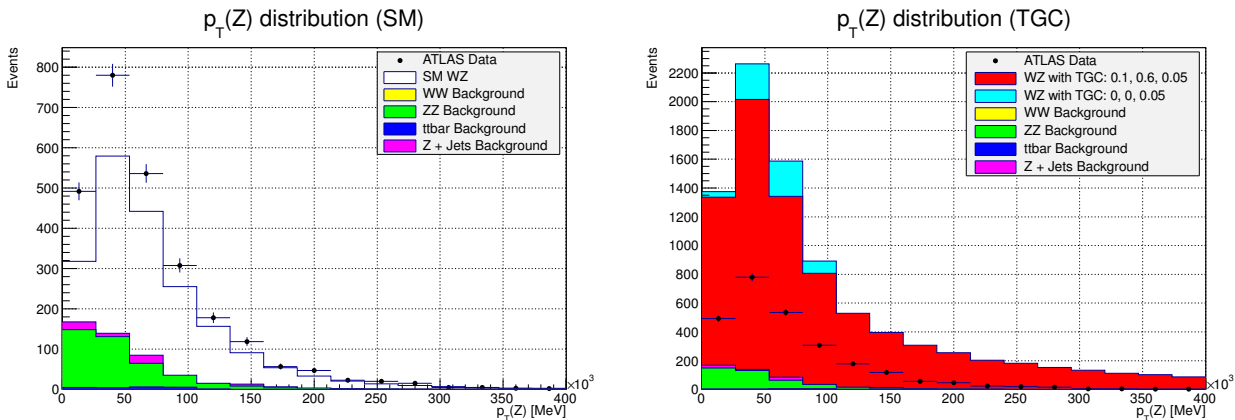
W reconstruction. The reconstruction of the W boson happens from the remaining lepton after the Z reconstruction, which is combined with the missing transverse energy \cancel{E}_T of the event.

When the electrons, muons and missing transverse energy \cancel{E}_T are extracted from the event, and the reconstruction requirements are fulfilled, it is then possible to combine it into a WZ pair.

Cut	Data	SM $W^\pm Z$	$W^\pm Z$ TGC 1	$W^\pm Z$ TGC 2
Event cleaning	33554445 ± 5793	205221 ± 126	60399 ± 64	60291 ± 64
Three leptons	4040 ± 67	2376 ± 13.5	9413 ± 25	8843 ± 24
$\cancel{E}_T > 20$ GeV	3058 ± 55	2090 ± 12.6	8480 ± 24	7852 ± 23
Z cut (Total)	2598 ± 51	1998 ± 12.4	8405 ± 24	7776 ± 23

Cut	ZZ	$t\bar{t}$	Z+jets	WW
Event cleaning	175984 ± 90.3	102667 ± 229	55365387 ± 10957	60 ± 1.6
Three leptons	1001 ± 6.8	62 ± 5.6	932 ± 45	2.3 ± 0.3
$\cancel{E}_T > 20$ GeV	540 ± 5	59 ± 5.5	531 ± 34	2.2 ± 0.3
Z cut (Total)	422 ± 4.4	24.3 ± 3.5	403 ± 29.6	0.9 ± 0.2

Table 2: A summary of the cut flow efficiency for the data samples and the Monte Carlo samples. ZZ , $t\bar{t}$, Z+jets and WW constitute the background MC samples. TGC 1 refers to the MC WZ sample simulated with $\Delta g_Z^1 = 0.1$, $\Delta \kappa_Z = 0.6$ and $\lambda_Z = 0.05$, while TGC 2 refers to the $\Delta g_Z^1 = 0$, $\Delta \kappa_Z = 0$ and $\lambda_Z = 0.05$ sample. Total events after cuts is 2598 ± 51 for data and 2848 ± 32.6 for SM WZ and background MC samples.

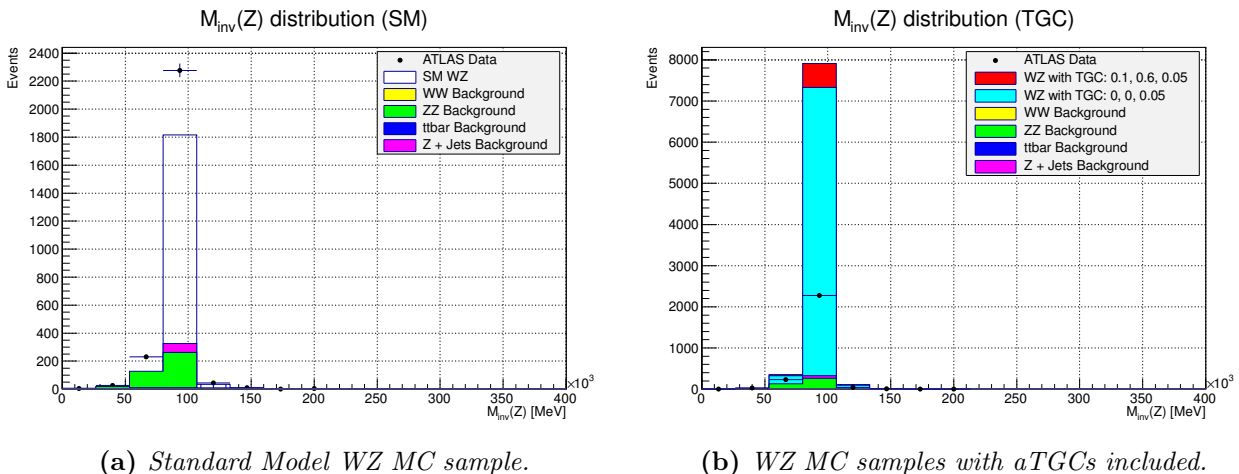


(a) Standard Model WZ MC sample.

(b) WZ MC samples with aTGCs included.

Figure 5: The $p_T(Z)$ distribution of all Monte Carlo simulations combined and compared with ATLAS data after the cut based selection. Most of the background is almost excluded, apart from the ZZ and Z+jets background. In (b) MC samples simulated to include TGCs by the event generator are shown. Red is for $\Delta g_Z^1 = 0.1$, $\Delta \kappa_Z = 0.6$ and $\lambda_Z = 0.05$, and cyan is for $\Delta g_Z^1 = 0$, $\Delta \kappa_Z = 0$ and $\lambda_Z = 0.05$. Notice that the histograms are not stacked but plotted individually.

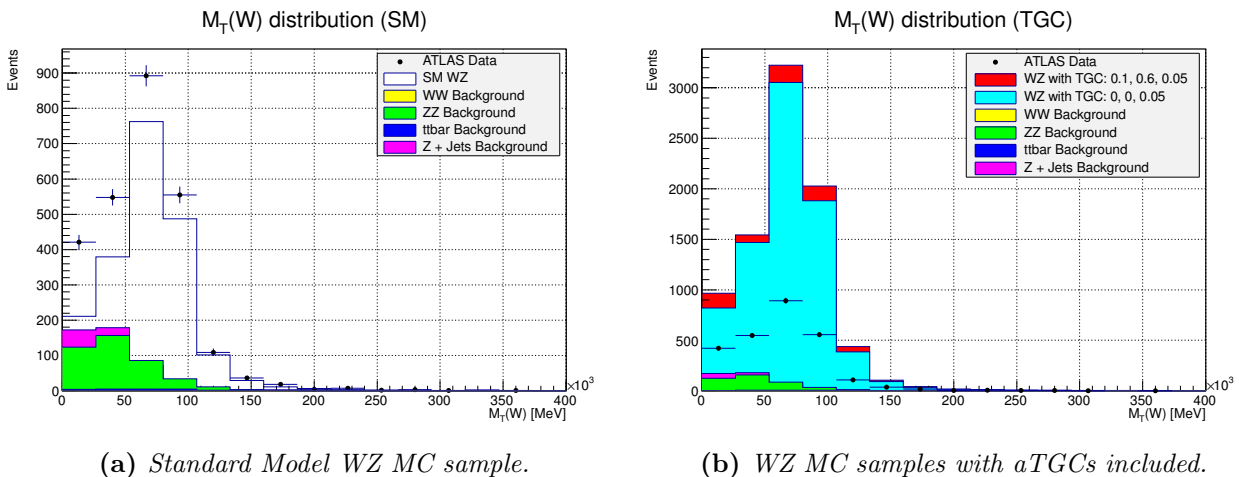
The performance of the event selection is seen in table 2. It is clear that almost all of the background is removed in the event selection and that the WZ dominates the final states. This is expected as this is the only process that will produce three leptons. In figure 5, the variable $p_T(Z)$ is shown after the cut based selection for both the Monte Carlo samples and data. In figure 6, the distribution of the invariant mass of the Z, $M_{inv}(Z)$, is shown and in figure 7 the transverse mass of the W, $M_T(W)$, is shown. A large boost in the MC samples with TGCs can be seen. This is due to the fact that the values selected for the parameters, the sample was simulated with, are quite large.



(a) Standard Model WZ MC sample.

(b) WZ MC samples with aTGCs included.

Figure 6: The invariant mass of the Z, $M_{inv}(Z)$, distribution of all Monte Carlo simulations combined and compared with ATLAS data after cuts. The peak is around 91 GeV as expected for the Z boson. In (b) MC samples simulated to include TGCs by the event generator is shown. Red is for $\Delta g_Z^1 = 0.1$, $\Delta \kappa_Z = 0.6$ and $\lambda_Z = 0.05$, and cyan is for $\Delta g_Z^1 = 0$, $\Delta \kappa_Z = 0$ and $\lambda_Z = 0.05$. Notice that the histograms are not stacked but plotted individually.



(a) Standard Model WZ MC sample.

(b) WZ MC samples with aTGCs included.

Figure 7: The transverse mass of the W, $M_T(W)$, distribution of all Monte Carlo simulations combined and compared with ATLAS data after cuts. The transverse mass has been calculated with $M_T(W) = \sqrt{2p_T(l_W)p_T(\nu_W)(1 - \cos(\phi(l_W) - \phi(\nu_W)))}$, from ref. [10]. The peak is situated around 80 GeV as expected for the W boson, with a large spread due to the use of missing transverse energy in the calculation. In (b) MC samples simulated to include TGCs by the event generator is shown. Red is for $\Delta g_Z^1 = 0.1$, $\Delta \kappa_Z = 0.6$ and $\lambda_Z = 0.05$, and cyan is for $\Delta g_Z^1 = 0$, $\Delta \kappa_Z = 0$ and $\lambda_Z = 0.05$. Notice that the histograms are not stacked but plotted individually.

4.3 Observables

A lot of different distributions will be investigated to see the effects of the anomalous triple gauge couplings. This makes it possible to determine which variables that are more sensitive to the anomalous couplings.

4.3.1 Optimal Observables

The usual method of measuring TGCs in high energy collisions has been a maximum likelihood fit of the transverse momentum distribution of one of the gauge bosons, $p_T(V)$, where $V = \{Z, W, \gamma\}$. There are two reasons for this: (1) the $p_T(V)$ distribution is very sensitive to anomalous TGCs as the distribution is sensitive to both angular and energy information, and (2) the $p_T(V)$ distribution is reconstructible without any assumptions or ambiguities. However, other statistical methods for deriving anomalous TGC measurements and confidence intervals exist, one of which is the method of Optimal Observable (OO). Some kinematic observables are more sensitive to anomalous TGCs than others and optimal observables are quantities with maximal sensitivity to the unknown coupling parameters. The method of Optimal Observables (OO) projects onto a single variable the kinematic information which is most sensitive to a particular anomalous TGC parameter. Each anomalous TGC has its own OO value. The OO value for a given λ coupling parameter of a particular event is given by:

$$OO(\lambda) = \lim_{\varepsilon_\lambda \rightarrow 0} \left(\frac{d\sigma(SM + \varepsilon_\lambda) - d\sigma(SM)}{\varepsilon_\lambda d\sigma(SM)} \right) \quad (39)$$

where $d\sigma$ is the differential cross-section for the event [11]. The OO value for a given coupling parameter is essentially the ratio between the coefficient of the linear term (from equation 35) for the coupling parameter and the coefficient for the SM. For the three couplings this will be

$$OO(\Delta g_1^Z) = \frac{F_1}{F_0}, \quad OO(\Delta \kappa_Z) = \frac{F_2}{F_0}, \quad OO(\lambda_Z) = \frac{F_3}{F_0} \quad (40)$$

for every event. Here the F coefficients come from equation 35 and we have $F_0 = d\sigma_{SM}$.

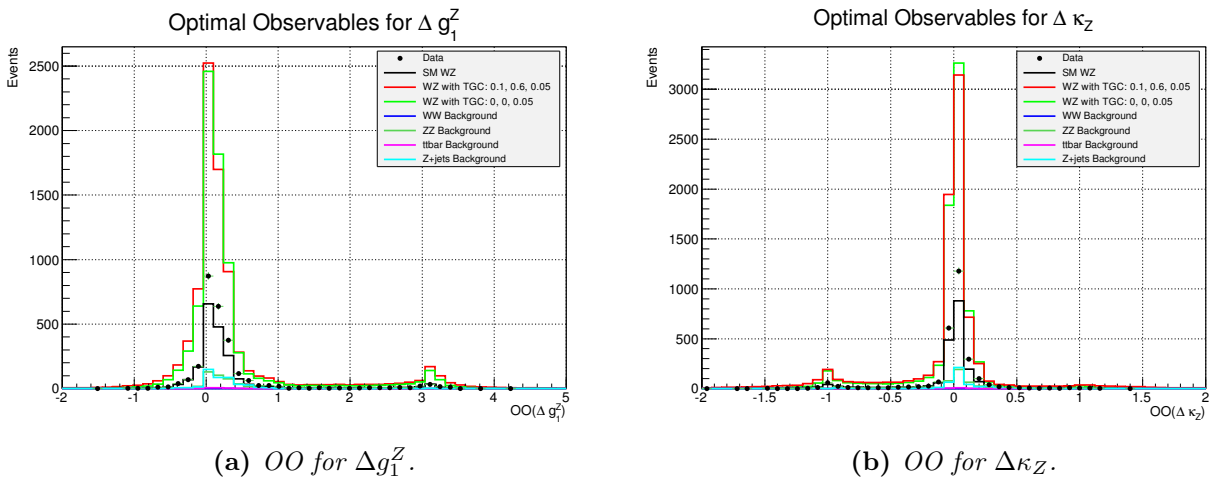


Figure 8: Optimal Observables for data compared with the MC samples. Notice that these histograms are not stacked but plotted individually.

5 Discussion

In table 2 the cut flow efficiencies are shown, where total events after cuts is 2598 ± 51 for data and 2848 ± 32.6 for SM WZ and background MC samples. The errors listed are statistical errors. Inclusion of systematic errors are necessary as well. The calculation of the cross-section used in the determination of the weight, includes a theoretical error in the range of 5-10%. In addition, the luminosity, which also appears in the calculation of the weights, includes an experimental error of around 3%.

In figure 8(a), 8(b), and 9 the Optimal Observables for the three anomalous coupling parameters are plotted for data compared with the MC samples. The effect non-standard couplings have on the OO distributions is clearly shown, as the OO for the MC samples simulated to include TGCs show strong sensitivity to the couplings (the green and red lines). The $OO(\Delta g_1^Z)$ distribution appears to be the least sensitive to the anomalous TGCs. The anomalous TGC parameters employed for the MC samples with simulated TGCs have been chosen so that the effect of the non-SM couplings are clearly visible, as is apparent on the figures. Data, however, seems to be very close to SM WZ with background. A comparison between the observables from figure 5, 6 and 7 among others and the Optimal Observables

can be made, to determine which of the observables are the most sensitive to the anomalous TGCs. To find the observables that are the most sensitive to the anomalous couplings, we can use the total significance, which is a measure of the signal-to-background ratio: $\text{Significance} = \frac{S}{\sqrt{S+B}}$, where the signal S are WZ events with TGCs and the background B is as described in section 4.2.1. This makes it possible to qualitatively see the difference between the SM and the distributions with anomalous TGCs. The couplings can be determined from the mean values of the Optimal Observables, $\langle OO \rangle$. A comparison of the mean values of the Optimal Observables values for the simulated TGC MC samples with the SM MC sample to see which sample correlates the most with the mean value of the OO value for data. A χ^2 test can be performed to compare mean of OO values with data, $\chi^2 = \frac{(\langle OO \rangle^{data} - \langle OO \rangle)^2}{\sigma_{OO,data}^2}$, where the smallest χ^2 value indicates the best fit [12]. A derivation of confidence limits from the Optimal Observables is possible. Confidence limits can be calculated for the anomalous TGCs by using a binned maximum likelihood fit to the OO distributions (see ref. [11]).

6 Conclusion

In this project the effects of the anomalous triple gauge boson couplings for the WWZ vertex with WZ final state have been investigated. By the use of the effective Lagrangian method, it has been possible to include the three non-SM couplings Δg_1^Z , $\Delta \kappa_Z$ and λ_Z . In the Standard Model (SM) the three parameters are zero. As seen on the histograms (figure 5, 6 and 7) and on the cutflow efficiency table (table 2) the ZZ and $Z + jets$ are the dominating background processes. But a mostly clean signal of WZ events was still obtained through appropriate selection cuts, of which the criteria of exactly three leptons was the one that made the largest cut in the data and MC samples. This was expected as WZ is the only process that will produce three leptons. It is found that the Optimal Observables for the three anomalous triple gauge couplings show strong sensitivity to the anomalous couplings. The $OO(\Delta g_1^Z)$ appeared to be the least sensitive to the anomalous parameters. Data, however, appears to closely favor a Standard Model without aTGCs, but the parameters for the MC samples simulated with TGCs were chosen to show a strong effect on observables. The method of Optimal Observables seem promising as competition to the commonly used $p_T(V)$ distribution. The LHC is scheduled to start again in 2015 with a collision energy of $\sqrt{s} = 14$ TeV. A larger collision energy would improve the ability to set limits on the TGC parameters and will open up a new, unexplored area, making the possibility to find New Physics (NP) in the near future look very promising.

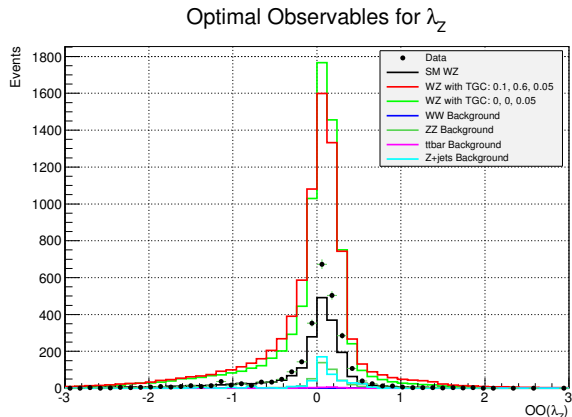


Figure 9: Optimal Observable for λ_Z . Plotted for data compared with the MC samples. Notice that these histograms are not stacked but plotted individually.

Bibliography

- [1] David Griffiths. *Introduction to Elementary Particles*. Wiley-VCH, Second, Revised Edition, 2012. ISBN 978-3-527-40601-2.
- [2] B.R. Martin and G. Shaw. *Particle Physics*. Wiley, Third Edition, 2012. ISBN 978-0-470-03294-7.
- [3] Goldstein, Poole and Safko. *Classical Mechanics*. Addison Wesley, Third Edition, 2002. ISBN 0-321-18897-7.
- [4] Morten Badensø. *Limits on Anomalous Triple Gauge Couplings in WW Production with Semileptonic Final State*. Master thesis, Niels Bohr Institute, January 2011.
- [5] Christian Bierlich. *Limits on triple gauge boson couplings*. Master thesis, Niels Bohr Institute, May 2012.
- [6] Website of the ROOT data analysis framework: <http://root.cern.ch/drupal/>
- [7] Rene Brun and Fons Rademakers. *ROOT User's Guide*. Cern, Geneva, 2007. Available at: <http://root.cern.ch/drupal/content/users-guide>
- [8] Website for the Sherpa MC event generator: <https://sherpa.hepforge.org/trac/wiki>
- [9] Website for the MC@NLO MC event generator: <http://www.hep.phy.cam.ac.uk/theory/webber/MCatNLO/>
- [10] DZero Collaboration. *A Measurement of the W Boson Mass*. December, 1997. [arXiv:hep-ex/9712928v1](https://arxiv.org/abs/hep-ex/9712928v1).
- [11] Matthew Dobbs. *Probing the Three Gauge-boson Couplings in 14 TeV Proton-Proton Collisions*. PhD thesis, McGill University, 1997.
- [12] M. Diehl and O. Nachtmann. *Optimal observables for measuring three-gauge-boson couplings in $e^+e^- \rightarrow W^+W^-$* . June, 1995. [arXiv:hep-ph/9603207v1](https://arxiv.org/abs/hep-ph/9603207v1).

A Appendix

A.1 Information on the Monte Carlo samples used

This appendix contains more detailed information on the Monte Carlo samples used for this study.

MCID	Process	Generator	k -factor	Δg_Z^1	$\Delta \kappa_Z$	λ_Z	Scale to 1fb^{-1}
129960-129977	WZ	MC@NLO	1.050	0.1	0.6	0.05	0.00334
129978-129995	WZ	MC@NLO	1.050	0	0	0.05	0.00334

Table 3: MC samples to model the signal, WZ . These samples are simulated to include TGCs.

MCID	Process	Generator	k -factor	Scale to 1fb^{-1}
126893	WZ	Sherpa	1.050	0.0037920

Table 4: MC sample to model the signal, WZ , from the Standard Model.

MCID	Process	Generator	k -factor	Scale to 1fb^{-1}
126894	ZZ	Sherpa	1.000	0.0022994
110001	$t\bar{t}$	MC@NLO and Jimmy	1.218	0.0253306
117650-117655	$Zee\text{Np}0\text{-}Zee\text{Np}5$	Alpgen and Pythia	1.000	0.1075531
117660-117665	$Z\mu\mu\text{Np}0\text{-}Z\mu\mu\text{Np}5$	Alpgen and Pythia	1.000	0.1075531
117670-117675	$Z\tau\tau\text{Np}0\text{-}Z\tau\tau\text{Np}5$	Alpgen and Pythia	1.000	0.1075531
126892	WW	Sherpa	1.050	0.0021385

Table 5: MC samples to model the background, ZZ , $t\bar{t}$, $Z + \text{jets}$ and WW .

The k -factor is the ratio of the NLO cross-section to the LO cross-section, used for reweighting of MC samples where a full NLO calculation would have been too CPU intensive.

In table 3, the scaling factors differed depending on the process that was simulated ($W^+Z \rightarrow l\nu ll$ or $W^-Z \rightarrow l\nu ll$). However for this study the samples for the processes were combined in one and hence, one scalefactor for both were needed. This was calculated by weighing the scalefactor for each process with the fraction of the corresponding cross-section (as the number of generated event were the same for both). The sum of the two weighted scalefactors is the quoted number in the table. The combination of the processes will introduce a small and non-significant error in the final result.

Zee , $Z\mu\mu$ and $Z\tau\tau$ refer to $Z+\text{jets}$, and $\text{Np}X$, where $X = 0 \dots 5$ refers to the number of additional partons in the final state. Each set with a different value of X had a different scaling coefficient (last column), but in the analysis the scale factor for the $\text{Np}0$ set was used for all of them as the difference was too small to be significant. This would introduce a small and nonsignificant error in the final results. The listed value for the scale to 1fb^{-1} for the $Z+\text{jets}$ rows is therefore the value for the $\text{Np}0$ set which was the used value.